

Lattice Design of a Low Emittance 100 TeV p-p Collider

1. Introduction

There is a renewed interest in a high-energy (100 TeV c.o.m.) p-p collider. R. Palmer came up with a concept [1] that significantly differs from the approach pursued by the FCC collaboration [2]. The major difference is a small transverse emittance which can be achieved using one of novel stochastic cooling techniques: either coherent electron cooling that uses electron beam as a probe and kicker, or optical stochastic cooling.

Small transverse emittance will permit to obtain the required luminosity with smaller number of protons per bunch and higher bunch sequence frequency thus solving the problem with the event pileup. Another advantage of small emittance is smaller transverse beam sizes allowing for smaller magnet apertures and/or lower β^* .

Another important difference is a lower dipole field in the arcs (8-9T) which optimizes the cost of the machine and alleviates problems associated with heat deposition by synchrotron radiation. At the same time this raises the question if the reduced radiative damping will be sufficient to overcome the IBS. To answer this question as well as how low β^* can be achieved a ring design is necessary.

In this report a first look at the lattice utilizing the advantages of R. Palmer's proposal is presented.

2. Beam parameters

Table 1 summarizes beam parameters proposed in [1]:

<i>Parameter</i>	<i>Unit</i>	<i>Value</i>
Beam energy, E	TeV	50
Protons/bunch, N_p	-	10^{10}
Transverse emittance, $\varepsilon_{\perp N}$	(π) mm·mrad	0.43
Longitudinal emittance, ε_{LN}	cm	6.4
Bunch length, σ_s	cm	5.5
Energy spread, σ_E/E	-	$2.2 \cdot 10^{-5}$
Bunch period	ns	5 (2.5)

For longitudinal emittance the LHC design value was taken, in CERN units it is $4\pi\varepsilon_{LN}m_p c = 2.5$ eV·s. The corresponding relative energy spread at the considered high energy is fairly small thus raising question of potential coherent instabilities. The most dangerous effect is switching off the longitudinal Landau damping due to incoherent synchrotron tune shift by wake fields [3]. We will use the analysis presented in the cited paper to estimate the instability threshold after the lattice parameters are established and justify the energy spread value of Table 1.

3. Interaction Region

To achieve the desired luminosity the beta-function at IP should be smaller than with other FCC proposals. On the other hand, smaller $\varepsilon_{\perp N}$ and N_p allow for a smaller crossing angle so that the required aperture of the final focus quads is not very large.

For the distance L^* from IP to the 1st quad we take twice the LHC value.

Table 2. IR parameters:

Parameter	Unit	Value
β^*	cm	5.5
full crossing angle, χ	μrad	145
L^*	m	46

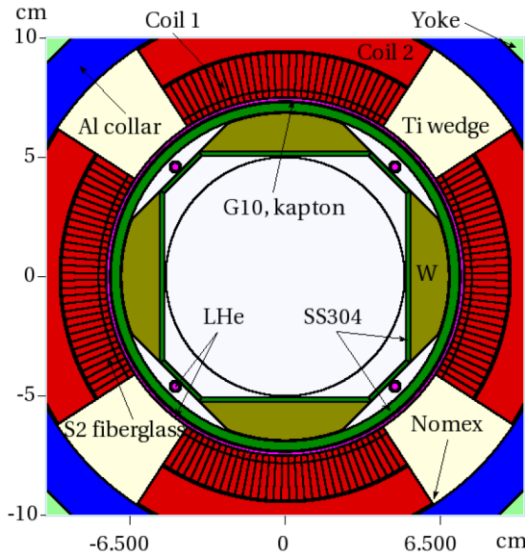


Figure 1: MARS model of the innermost region of the HL-LHC Q1 quadrupole distance from the IP.

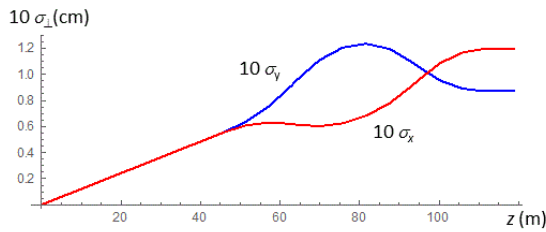


Figure 2: Beam envelopes vs distance from IP

for in a self-consistent way. Thus found beam sizes in the inner triplet are shown in Fig.2. The maximum value of the beta function is 188.7 km.

Table 3. The IR quadrupole parameters.

Parameter	Q1	Q2	Q3
Gradient, T/m	285.7	284.0	258.4
Aperture, mm	84	84	94
Number of sections	3	5	3
Section length, m	5.4	5.6	5.4

The cited apertures do not provide additional room for orbit errors (on top of $10\sigma_{\perp}$ clearance).

The quadrupoles are supposed to be cut in sections no longer than 6 m with 30cm gaps between them (this takes into account $\sim 2b$ difference between physical and magnetic length, b being the bore radius, and at least 8cm thick endplates). Distance between such groups of quads was set at 1 m.

Determining the required quadrupole aperture we follow the design proposed for HL-LHC [4] which is shown in Fig. 1 for the HL-LHC 1st quad.

In the LHC case the difference between the quad bore and the beam pipe radii is 2.5 cm, the W absorber thickness being 1.5 cm. Here we increase it by 1 cm for the first section of Q1 so that the bore-pipe radii difference is initially 3.5 cm and then tapered down to the same 2.5 cm in the last Q1 section. Determining the bore radius b we assume that the beam pipe radius is at least $\chi \cdot z / 2 + 10 \text{ Max}(\sigma_x, \sigma_y)$, where z is

The most important guess is what quad tip field can be achieved in the near future. We take a modest value of $B_{\text{tip}} = 12 \text{ T}$ despite the more optimistic prognosis of 13 T with >20% operational margin for Nb_3Sn technology [5]. With HTS $B_{\text{tip}} = 16 \text{ T}$ is probably achievable.

Quadrupoles parameters satisfying the above requirements and the optics functions were sought

4. Arc and Matching Section

Large beta function values in the IR quadrupoles make the multipole errors in these quads potentially very dangerous. Nonlinear correctors of these errors can be placed only where the beams are separated to avoid the feeddown effect. We keep beta functions \sim constant over the separation region (Fig. 3) to make these correctors more efficient – this is a major difference with other FCC IR designs. Small beta function slope also minimizes kinematic nonlinearities and the dispersion invariant generated by separation bends. Further studies will show if this innovation is really helpful.

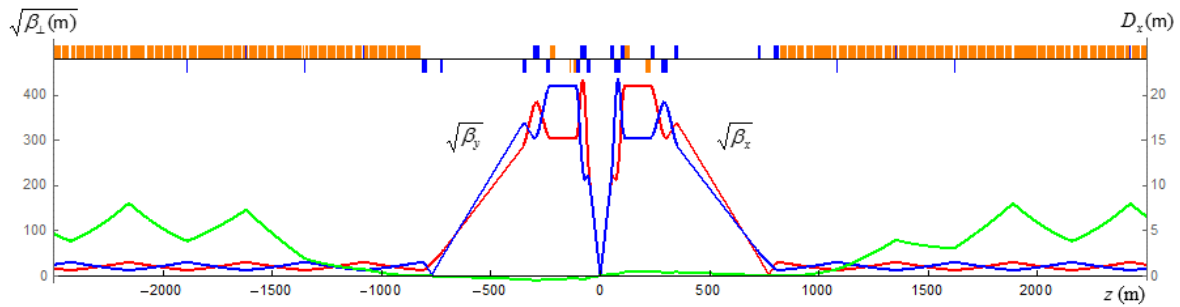


Figure 3: Optics functions and layout of IR, matching section, dispersion suppressor and the 1st arc cell on each side of IP. Bends are shown in orange, quads in blue.

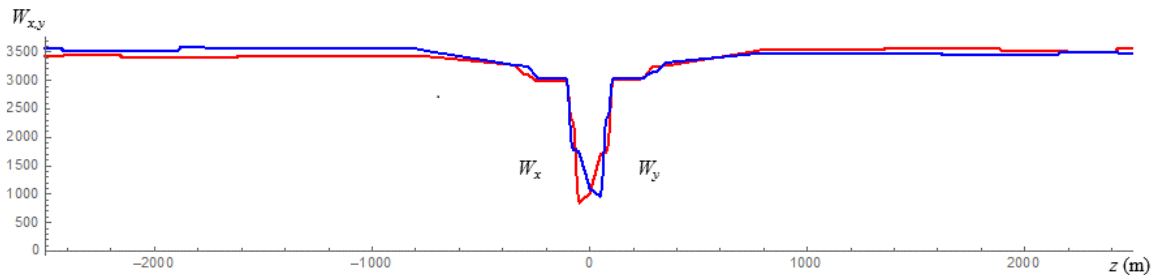


Figure 4: Montague chromatic functions as found.

For the arcs we use regular $90^\circ/90^\circ$ FODO cells with length 536 m chosen to keep $\beta_{\max} < 1\text{ km}$ (actual value being $\beta_{\max} = 912.5\text{ m}$). There are 74 bending magnets per cell having 6 m length and 8.35 T field. The number of full cells per arc is 141. For the dispersion suppressor we chose the classical 2-cell scheme which allows for exact matching of the dispersion and its slope for the two beams.

The ring layout is simplified in this study, it has just 2 opposite low-beta insertions. The full length of the ring is 158.7 km.

The most detrimental effects associated with low β^* come from chromatic perturbations. With 2 IPs it is possible to achieve their cancellation if the phase advances between IPs are an odd multiples of $\pi/2$. Then the overall tunes will be half-integer which is beneficial for orbit stability and dynamic aperture. We chose the fractional tunes 0.425, 0.415 which are a mirror reflection of the well-tested Tevatron tunes. The integer part of the tunes for the chosen number of arc cells is 74.

As found values of the Montague chromatic functions are shown in Fig. 4. Thanks to small energy spread the β -functions variation at $1\sigma_E$ is just 2.4% at IPs and about 8% in the arcs, so from this point of view there is no need in splitting focusing and defocusing sextupoles into subfamilies.

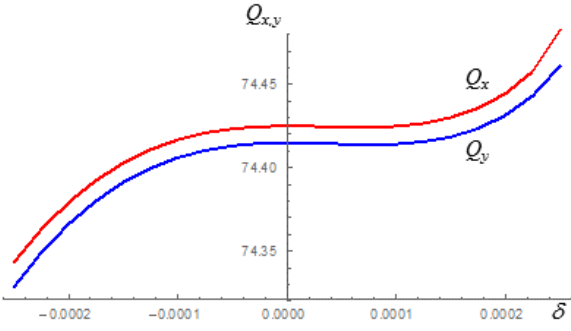


Figure 4: Tunes vs relative momentum deviation

However, it is the higher order chromaticity which is most detrimental. Figure 5 shows dependence of the tunes on the relative momentum deviation. It is dominated by the third derivative:

$Q_x'''=2.72 \cdot 10^{10}$, $Q_y'''=2.57 \cdot 10^{10}$. In principle, the third order chromaticity can be corrected with decapoles in the arcs, but the required strength is very large. On the other hand, the stable momentum range (-0.0004, +0.00025) seems sufficient owing to small energy spread. If further studies will indicate that it is not really so then

introduction of special "chromatic correction sections" must be considered.

Sextupole strength needed for linear chromaticity correction is quite low, therefore - with higher order chromaticity left untouched - the on-momentum dynamic aperture in ideal lattice is large. The fringe fields are unlikely to drastically reduce it since the IR quad apertures are rather small.

Table 4. Basic parameters of the lattice:

Parameter	Unit	Value
Circumference, C	km	158.7
Number of IPs	-	2
Tunes, $Q_x / Q_y / Q_s$	-	74.425 / 74.415 / 0.00224
Momentum compaction, α_c	-	$2.22 \cdot 10^{-4}$
Stable momentum range	%	-0.04, +0.025
RF voltage @ 400 MHz	MV	33.6
Radiation damping times	s	$2.2 \cdot 10^4 / 2.2 \cdot 10^4 / 1.1 \cdot 10^4$
IBS lifetimes	s	$5.2 \cdot 10^4 / NA / 2.5 \cdot 10^5$
Natural energy spread	-	$3.8 \cdot 10^{-6}$
Peak luminosity	$s^{-1}cm^{-2}$	$2.7 \cdot 10^{35} (5.4 \cdot 10^{35})$

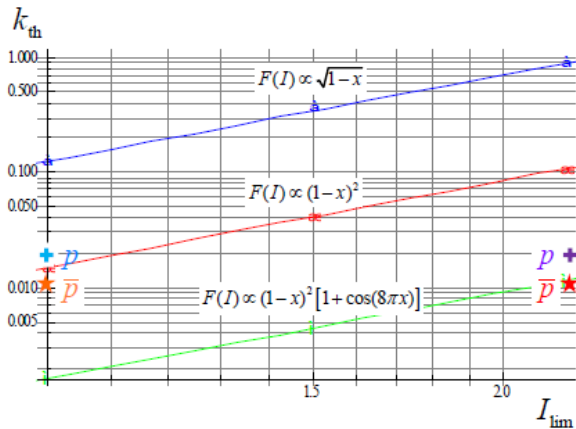


Figure 5: Threshold intensity parameter vs limiting action value (borrowed from Ref. [3])

5. Longitudinal stability

To estimate the instability threshold due to loss of the longitudinal Landau damping we will use theory developed in [3]. In dimensionless units employed in that paper the emittance is

$$\varepsilon_B = \varepsilon_{LN} \frac{2\pi\alpha_c h^2}{\gamma Q_s C} = 0.215 \quad (1)$$

where γ is relativistic mass factor, $h=211746$ is the RF harmonic number. Assuming that the distribution is effectively truncated just at 2σ we have for the limiting value of the action variable

$$I_{lim} = 4\varepsilon_B = 0.86 \quad (2)$$

Using scaling law established in [3], $k_{th} \sim I_{lim}^{5/2}$, we obtain by extrapolation of the middle curve in Fig.5 $k_{th}=0.01$ or, for the threshold impedance

$$\left| \frac{Z_n}{n} \right|_{th} = \frac{30 \gamma Q_s^2 C}{N_p r_p \alpha_c h^3} k_{th} = 0.38 \Omega \quad (3)$$

where r_p is classical proton radius. This value is twice the FFC impedance estimate so that there seem to be no problem with small energy spread cited in Table 1.

The author is grateful to A. Burov, N. Mokhov, I. Rakhno and R. Palmer for helpful discussions.

6. References

- [1] R.B. Palmer et al., Accelerator and optimization issues for a 100 TeV pp collider (2015, unpublished)
- [2] <https://fcc.web.cern.ch/>
- [3] A. Burov, <http://accelconf.web.cern.ch/AccelConf/PAC2011/papers/MOODS4.PDF>
- [4] N. Mokhov, I. Rakhno et al. FERMILAB-PUB-15-095-APC, 2015.
- [5] A. Zlobin, private communication